Task 5 and 6 Report

Group Members: Antonia Aanesen, Teodor V. Fossdal

October 2025

Task 5

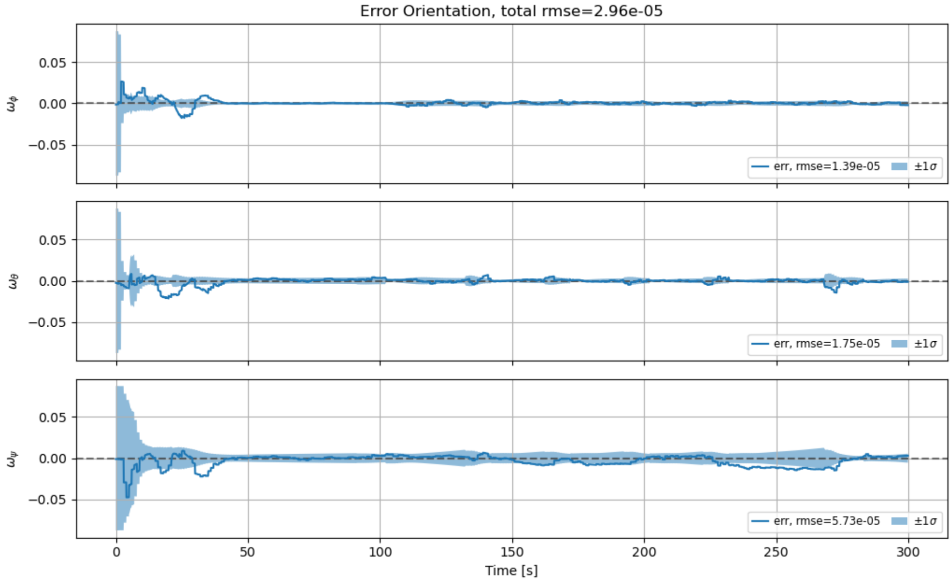

Figure 1: Error orientation over time

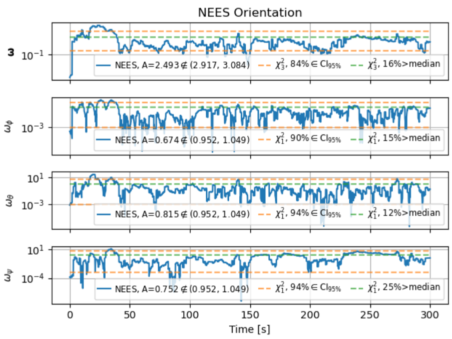

(a) NEES for simulated data

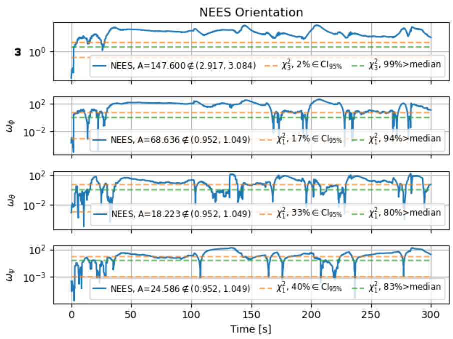

(b) NEES for simulated data with integer rounded corrections

Figure 2: NEES plots for normal simulated data and simulated data with integer roundings for corrections

Orientation errors

In Figure 1 we can see that the estimated error does not converge. This occurs even though the covariance is constant, since we do not measure orientation at any point, only estimate it, as it is unobservable. We then get no corrections on the orientation. The gravity vector and IMU can be used to infer roll and pitch, but there is no measurement giving information on yaw. For this reason yaw has the biggest error.

The fact the yaw is unobservable and we get no corrections means that both the true error and the estimated error may continue to grow, and could grow indefinitely if we do not anything to correct it. An example of something that help remedy this problem is a type of compass.

Rounded corrections

When introducing integer rounding to our gyro and accelerometer corrections we get much bigger errors. We no longer account for these small variations, and our filter is no longer fed random, zero mean data.

Tuning

Three different changes were tested to look at how different changes effect the errors and results.

Downsampled IMU

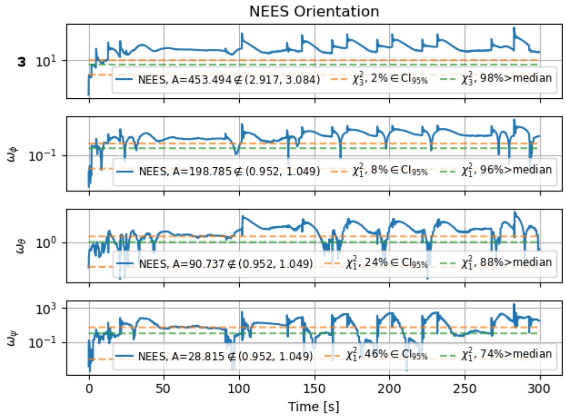

(a) NEES

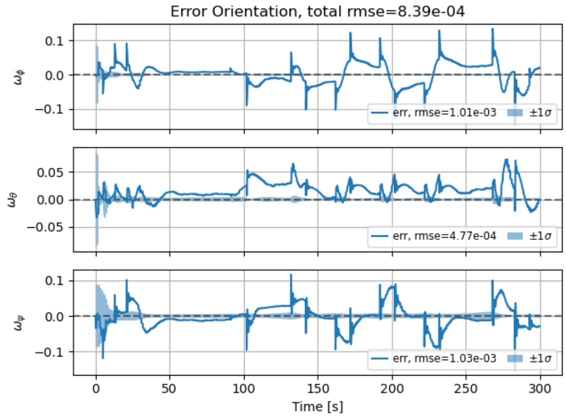

(b) Orientation RMSE

Figure 3: Plots showing the NEES and RMSE of the orientation when the IMU is downsampled from 100 Hz to 10 Hz.

The first change made is downsampling of IMU measurements from 100 Hz to 10 Hz. We can observe from Figure 3a that the filter becomes overconfident, trusting its prediction to much. This is because the filter has measurements to use as inputs for prediction, but does not gain as much information from these measurements as it should , as they are too infrequent. We can also see when comparing Figure 3b to Figure 1 that the RMSE increases by approximately two decades, as the filter has less measurements, and therefore less information, to work with.

Downsampled GNSS

Interestingly, we do not see this same effect when downsampling the GNSS measurements used for correction. Figure 4a shows that the filter is not noticeably more nor less confident than the original case, shown in Figure 2a. This is also true for the RMSE, where Figure 4b shows that it sits at approximately 10^{-5}, just as in Figure 1. We can see that having enough IMU measurements for prediciton is vital, while we can do with a bit less GNSS measurements for correction.

Wrong initial nominal state

Lastly, setting the initial value for the nominal yaw state to $\pi/2$, rather than the correct value 0, change the behaviour of the filter initially, but we can see that the filter recovers with time, converging on the error and neither being over- nor underconfident. This happens even though the error state then starts out large and is based on linearisation.

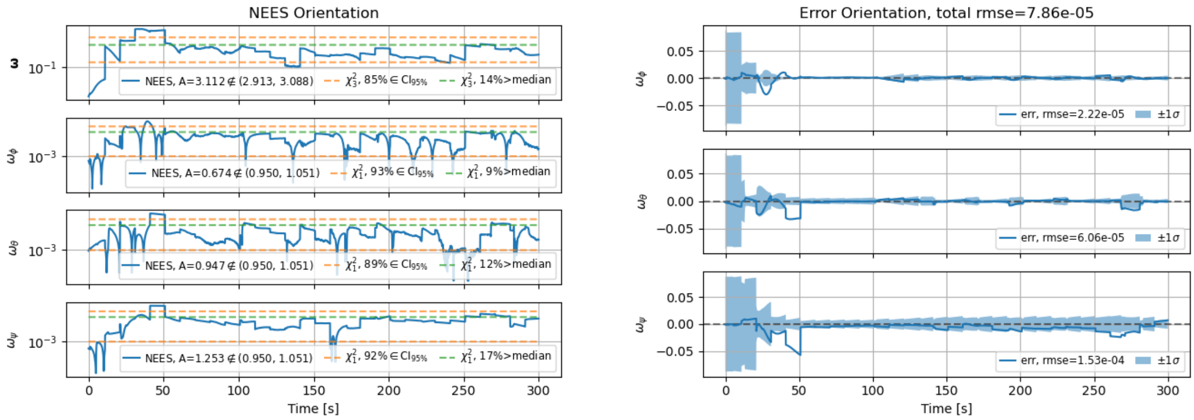

(a) NEES (b) Orientation RMSE

Figure 4: Plots showing the NEES and RMSE of the orientation when the GNSS is downsampled from 1 Hz to 0.1 Hz.

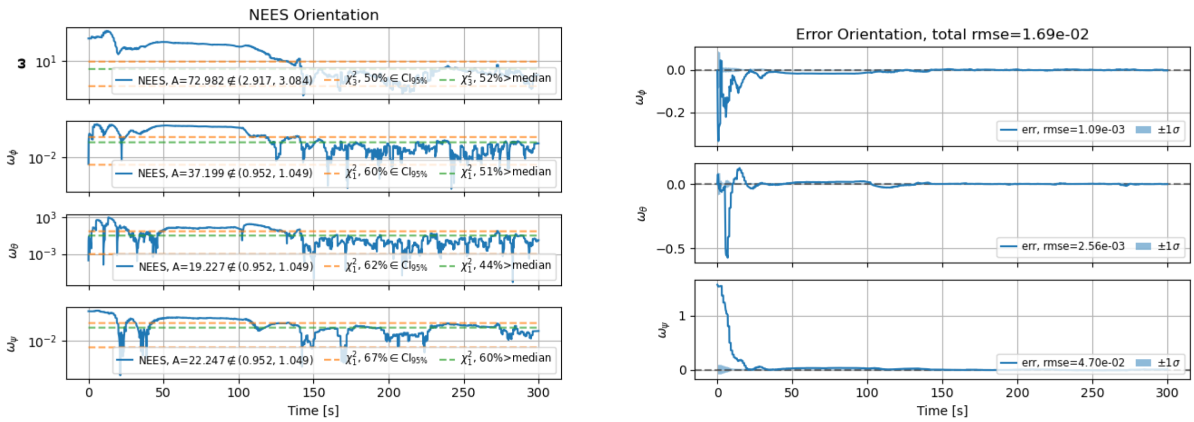

(a) NEES (b) Orientation RMSE

Figure 5: Plots showing the NEES and RMSE of the orientation when the initial nominal state yaw is completely wrong

Task 6

Asynchronous measurements

The IMU measurement is used as a control input in the ESKF, and arrives at $t_{\text{IMU},k}$ and $t_{\text{IMU},k+1}$. When recieving a GNSS measurement at say $t_{\text{GNSS},\kappa}$, where $t_{\text{IMU},k} < t_{\text{GNSS},\kappa} < t_{\text{IMU},k+1}$, one may use the IMU measurement from $t_{\text{IMU},k}$ and the time interval between $t_{\text{IMU},k}$ and $t_{\text{GNSS},\kappa}$ to predict the measurement at $t_{\text{GNSS},\kappa}$, do injection using the GNSS measurement, and then again use the IMU measurement to predict from $t_{\text{GNSS},\kappa}$ to the the next IMU measurement at $t_{\text{IMU},k+1}$.

Rounded corrections

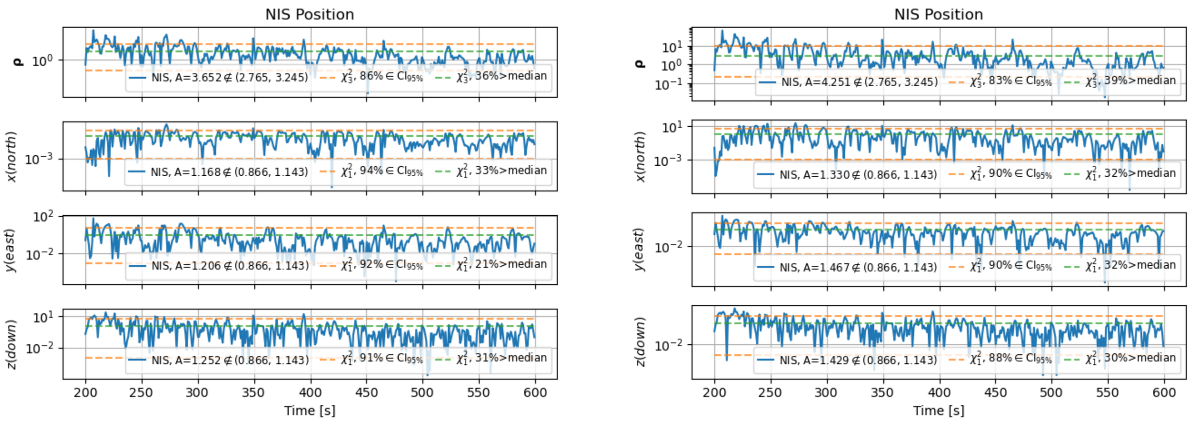

(a) NIS without integer rounding

(b) NIS with integer rounding

Figure 6: Comparison of NIS values with and without integer rounding of correction matrices.

When using integer rounding on the corrections for the real data, rather than the sim data, we see only a very small change in the NIS. We do not see significantly worse results, even by introducing this larger model mismatch. We need to to the calibration, but this seems to indicate that this calibration is of lesser importance, contrary to our intuition.

Tuning

Three changes were made to the system to test out how different changes effects the filter. We changed the GNSS measurement noise, the covariance of the IMU measurements and how fast the error from biases converges to zero.

Increased GNSS noise

The first change made was changing the GNSS measurement noise `gnss-std-ne` from 0.3 to 10.3 and `gnss-std-d` from 0.5 to 10.5. We can see in Figure 7a that the filter becomes underconfident, and we can also see from Figure 7b larger deviations between the measured GNSS position and the estimated position. The increased noise on the GNSS measurement increases the difference between prediction and measurement, and the filter starts to trust less in its own predictions.

Reduced IMU process noise

Next up the process noise of the IMU was decreased by three decades to model the IMU being deterministic, rather than random. The model now ignores the fact that the IMU measurements are noisy, and becomes overconfident as seen in Figure 8a. We do not, however, observe much

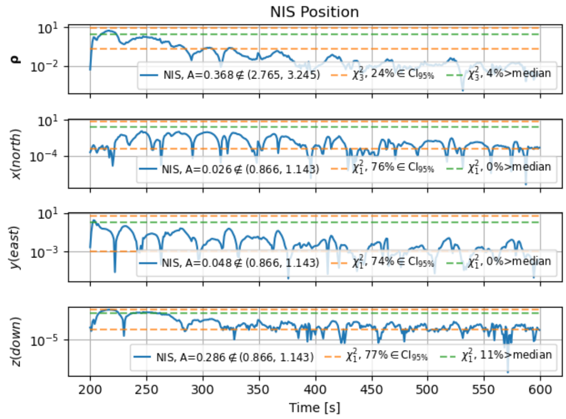

(a) NIS plot

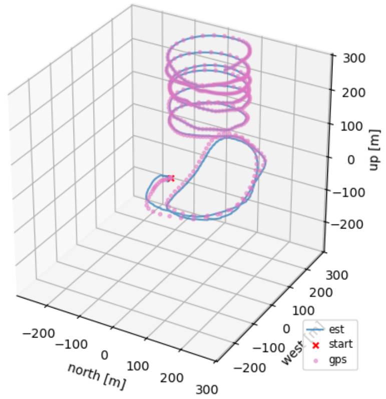

(b) 3D Position

Figure 7: NIS and 3D position when GNSS is unreliable.

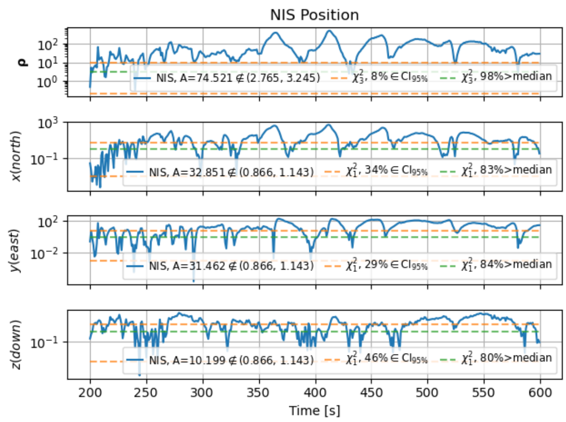

(a) NIS plot

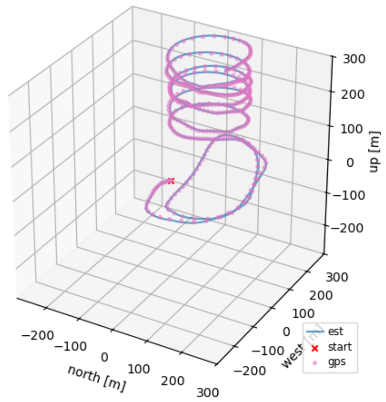

(b) 3D Position

Figure 8: NIS and 3D position when the IMU is modeled as deterministic.

of an increased deviation between the GNSS measurements and the estimated position, possibly because the frequency of the predictions are too high to be spotted in the plot.

Quick bias convergence

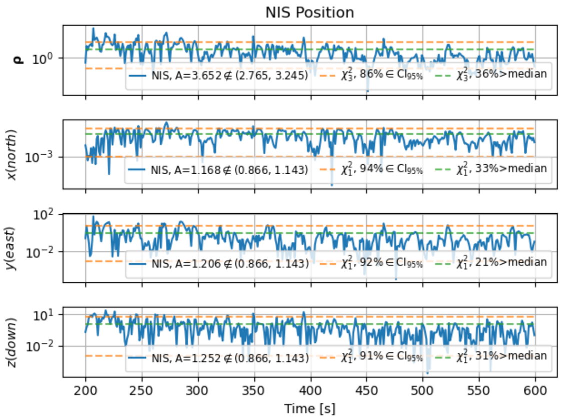

(a) NIS plot

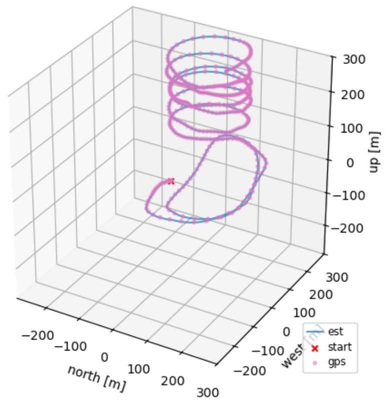

(b) 3D Position

Figure 9: NIS and 3D position when the error from bias is modelled as converging quickly.

The last change made was decreasing the time constant of the dynamics of the bias estimation from Equation 10.50 in Brekke [2025], such that the bias is modelled as rapidly going to zero. This results in the filter increasing process noise and "forgetting" previous bias information, as the filter assumes the bias may change rapidly. Figure 9a show that the filter is a little overconfident, but the estimated position and the GNSS measurements seem to still match quite well for the 3D position shown in Figure 9b.

References

Edmund Førland Brekke. Fundamentals of sensor fusion, 2025.